Non-Markovian entanglement dynamics of three independent qubits within atomic-cavity system

J S Kosasih[1,2], **V A Wasesatama**[1,a]

[1] Theoretical High Energy Physics Research Division, Department of Physics, Faculty of Mathematics and Natural Sciences, Institut Teknologi Bandung, Jl. Ganesha 10 Bandung 40132, Indonesia
[2] Indonesia Center for Theoretical and Mathematical Physics (ICTMP), Jl. Ganesha 10 Bandung 40132, Indonesia

E-mail: [a]vincentius.aryo@students.itb.ac.id

Abstract. All realistic quantum systems will interact with their environments. This fact presents challenges to the implementation of quantum systems for practical systems. One of the most important quantum resources is the implementation of entanglement. In this paper, we investigate the interplay between the effects of noisy environments and the dynamics of entanglement. The open quantum system model that will be used is cavity quantum electrodynamics (CQED) with three-qubit interacting independently with a variation of environmental model. We use master equation to describe the dynamics of the open quantum system and a lower bound concurrence (C_{LBC}) to measure the entanglement of tripartite qubit. We derive the exact dynamics of each model and use C_{LBC} method proposed by Li et.al to visualize entanglement dynamics. By adjusting the environmental parameters, we also found revivals and dark-periods of entanglement which are unique to non-Markovian processes.

1. Introduction

Quantum information and computation is deemed as the next revolution in information technology and genuine entanglement is its indispensable and most valuable ingredient and resource [1]. The quantumness of entangled states have been exploited for the popular teleportation and dense coding [2] to quantum error correction [3], and the understanding of the dynamical evolution of entanglement will prove valuable for its vast and far-reaching applications potential. The characterization of entanglement is one of many problems that must be confronted by the researchers in implementing entanglement as information resource. Maintaining and controlling entanglement also present obstacles that must be overcome, since it is related to practical questions about the robustness of many quantum computing and information processing technologies. This problem will be aggravated for systems in contact with the environment, which in practice is unavoidable for all quantum systems. For multipartite quantum systems, interaction with environment not only will change local properties of the systems but also global properties like the entanglement between the subsystems. Careful analysis of the interplay between the effects of noisy environments and the dynamics of entanglement may help us understand the foundation of quantum systems better and can reveal the underlying requirements for building workable quantum computers.

In this paper, we investigate the entanglement of qubits interacting with electromagnetic modes inside a lossy cavity commonly referred to as the cavity quantum electrodynamics (CQED) model. In the last two decades, many applications and architectures have been developed using the CQED model both from theoretical [4] and experimental [5] perspectives. It is then interesting to see the entanglement dynamics of this noisy system especially for multipartite qubits that offer much more power as information resources [6]. We describe each and total qubit in cavity dynamics analytically using Bellomo procedures [7] and visualized entanglement evolution using lower bound concurrence by Li et al. [8] as a measure. We will consider three different models of environment each differ by which qubits are inside the cavity.

This paper is organized as follows. In section 2 we solve exact evolution dynamics for atom-cavity mode with Lorentzian spectral density to obtain dynamical density matrix for each qubit. Section 3 introduces the procedure to obtain the composite reduced density matrix for three qubits with entangled initial states and the methodology to measure its entanglement. In section 4 we calculate entanglement evolution for each environment model. We summarize our result in section 5.

2. Model and Qubit Dynamical Calculation

We will consider systems of three two-level subsystems where each qubit either interacts with its own environment or is isolated from the external environment. The three qubits are initially in the state of maximally entangled and spatially separated. We consider three types of systems illustrated in Figure 1. A single qubit coupled to the cavity is described by the Hamiltonian

$$\hat{H} = H_S + H_B + H_I, \tag{1}$$

where in the RWA we have Jaynes-Cummings Hamiltonian

$$\begin{aligned} H_S = \frac{1}{2}\hbar\omega_0\sigma_z, \quad H_B = \hbar\sum_k \omega_k b_k^\dagger b_k, \\ H_I = \hbar\sum_k g_k\sigma_+ b_k + g_k^*\sigma_- b_k^\dagger, \end{aligned} \tag{2}$$

where ω_0 is the transition frequency between the two levels, $\sigma_\pm$ is the raising and lowering operators of the qubit, g_k is the coupling strength between system and the cavity for single excitation with frequency ω_k, and b_k and b_k^+ are annihilation and creation operators of the cavity, respectively.

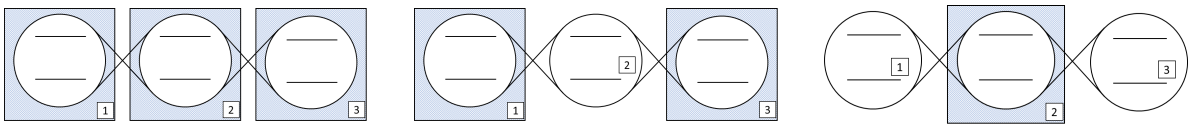

(a) Three-Cavity System (b) Two-Cavity System (c) One-Cavity System

Figure 1: Environment Models

We will use the subscript os (cs) to denote the evolution of the open system (closed system). From the Hamiltonian (1), exact dynamics of the qubit system can be obtained by solving the Schrödinger equation for the total system in the interaction picture,

$$\frac{\mathrm{d}}{\mathrm{d}t}\left|\psi_{os}(t)\right\rangle = -iH_I\left|\psi_{os}(t)\right\rangle, \tag{3}$$

with all possible qubit-cavity states are,

$$|\psi_{os}(t)\rangle = c_0(t)\,|0\rangle_S \otimes |\mathbf{0}\rangle_R + c_1(t)\,|1\rangle_S \otimes |\mathbf{0}\rangle_R + \sum_k c_k(t)\,|0\rangle_s \otimes |\mathbf{1}_k\rangle_R \tag{4}$$

and setting initial condition as

$$|\psi_{os}(0)\rangle = c_0(0)\,|0\rangle_S \otimes |\mathbf{0}\rangle_R + c_1(0)\,|1\rangle_S \otimes |\mathbf{0}\rangle_R\,, \tag{5}$$

where $|\mathbf{0}\rangle = |00\ldots00\rangle$ is the state when there is no excitation in the cavity and $|\mathbf{1}_k\rangle = |00\ldots1\ldots00\rangle$ is the state containing one photon in mode k.

As it is with lossy systems we can assume the excited photon in the cavity be either re-excite the qubits or dissipate to the larger environment. Then the bath state can be taken as a stationary vacuum state $\rho_B(t) \approx \rho_B = |0\rangle\langle 0|$and the reduced density matrix of the qubits as

$$\rho_S = tr_B(|\psi(t)\rangle\langle\psi(t)|) = \begin{pmatrix} |c_1(t)|^2 & c_0(t)c_1^*(t) \\ c_1(t)c_0(t) & 1-|c_1(t)|^2 \end{pmatrix}. \tag{6}$$

Substituting (4-5) to solve the Schrödinger equation (3) we calculate the dynamical coefficient $c_1(t)$ and $c_0(t)$

$$\begin{aligned} \frac{\mathrm{d}}{\mathrm{d}t}|\psi_{os}(t)\rangle &= \frac{\mathrm{d}}{\mathrm{d}t}c_0(t)\,|0\rangle_S \otimes |\mathbf{0}\rangle_R + \frac{\mathrm{d}}{\mathrm{d}t}c_1(t)\,|1\rangle_S \otimes |\mathbf{0}\rangle_R + \sum_k \frac{\mathrm{d}}{\mathrm{d}t}c_k(t)\,|0\rangle_s \otimes |\mathbf{1}_k\rangle_R \\ &= -i\sum_k g_k\sigma_+ b_k e^{-i(\omega_k-\omega_0)t} + g_k^*\sigma_- b_k^\dagger e^{i(\omega_k-\omega_0)t} \times \Big(c_0(t)\,|0\rangle_S \otimes |\mathbf{0}\rangle_R \\ &\qquad + c_1(t)\,|1\rangle_S \otimes |\mathbf{0}\rangle_R + \sum_l c_l(t)\,|0\rangle_s \otimes |\mathbf{1}_l\rangle_R\Big) \end{aligned} \tag{7}$$

$$\begin{aligned} &\frac{\mathrm{d}}{\mathrm{d}t}c_0(t)\,|0\rangle_S \otimes |\mathbf{0}\rangle_R + \frac{\mathrm{d}}{\mathrm{d}t}c_1(t)\,|1\rangle_S \otimes |\mathbf{0}\rangle_R + \sum_k \frac{\mathrm{d}}{\mathrm{d}t}c_k(t)\,|0\rangle_s \otimes |\mathbf{1}_k\rangle_R = \\ &\quad = -i\sum_k \Big(g_k^* c_1(t)e^{i(\omega_k-\omega_0)t}\,|0\rangle_s \otimes |\mathbf{1}_k\rangle_R - \sum_l \delta_{lk} g_k c_l(t) e^{-i(\omega_k-\omega_0)t}\,|1\rangle_S \otimes |\mathbf{0}\rangle_R\Big). \end{aligned} \tag{8}$$

Compare both side of equation (8), the differential equation for the dynamical coefficient are

$$\begin{aligned} \frac{\mathrm{d}}{\mathrm{d}t}c_0(t) &= 0, \\ \frac{\mathrm{d}}{\mathrm{d}t}c_1(t) &= -i\sum_k g_k c_k(t) e^{-i(\omega_k-\omega_0)t}, \\ \sum_k \frac{\mathrm{d}}{\mathrm{d}t}c_k(t) &= -i\sum_k g_k^* c_1(t) e^{i(\omega_k-\omega_0)t}, \end{aligned} \tag{9}$$

and its solutions

$$\begin{aligned} c_0(t) &= c_0(0), \\ c_k(t) &= -i\int_0^t g_k^* c_1(s) e^{i(\omega_k-\omega_0)s} ds. \end{aligned} \tag{10}$$

Substitute solution (10) to equation (9) to get the solution for $c_1(t)$

$$\begin{aligned} \frac{\mathrm{d}}{\mathrm{d}t}c_1(t) &= -\sum_k |g_k|^2 \int_0^t c_1(s) e^{i(\omega_k-\omega_0)s} e^{-i(\omega_k-\omega_0)t} ds, \\ &= -\int_0^t \sum_k |g_k|^2 c_1(s) e^{i(\omega_0-\omega_k)(t-s)} ds. \end{aligned} \tag{11}$$

Taking the limit of infinite cavity mode, one finds that the dynamic of the system is fully characterized by the spectral density describing the correlation function of the environment observable,

$$\begin{aligned} \langle B(t)B(s)\rangle_B &= \sum_k |g_k|^2 e^{-i\omega_k(t-s)}, \\ \sum_k |g_k|^2 e^{i(\omega_0-\omega_k)(t-s)} &= \langle B(t-s)B(0)\rangle_B e^{i\omega_0(t-s)} = \int_{-\infty}^{\infty} J(\omega) e^{i(\omega_0-\omega)(t-s)} d\omega. \end{aligned} \tag{12}$$

Here we will use the following spectral density $J(\omega)$ which describes a typical imperfect/lossy cavity supporting one mode ω_0 in the vacuum state,

$$J(\omega) = \frac{1}{2\pi} \frac{\gamma_0 \lambda^2}{(\omega_0 - \omega) + \lambda^2}, \tag{13}$$

where γ_0 is the microscopic system-cavity coupling constant and λ defines the spectral width of the coupling. The parameter γ_0 is related to the relaxation time τ_R^{-1} and λ is related to the bath correlation time τ_B^{-1} [9]. Using spectral density (13), equation (12) can be calculated with complex integral and residue theorem,

$$\int_{-\infty}^{\infty} \frac{1}{2\pi} \frac{\gamma_0 \lambda^2}{(\omega_0 - \omega) + \lambda^2} e^{i(\omega_0-\omega)(t-s)} d\omega = \frac{1}{2} \gamma_0 \lambda e^{-\lambda|t-s|}. \tag{14}$$

It follows that equation (11) can be rewritten as,

$$\frac{\mathrm{d}}{\mathrm{d}t} c_1(t) = -\int_0^t \frac{1}{2} \gamma_0 \lambda e^{-\lambda|t-s|} c_1(s) ds. \tag{15}$$

And its solution using Laplace transformation,

$$c_1(t) = c_1(0) e^{-\frac{\lambda t}{2}} \left(\cosh\left(\frac{gt}{2}\right) + \frac{\lambda}{g} \sinh\left(\frac{gt}{2}\right) \right), \tag{16}$$

with,

$$g = \sqrt{\lambda^2 - 2\lambda\gamma_0}. \tag{17}$$

The dynamical density matrix representation, equation (6), is then given by

$$\rho_{os}(t) = \begin{pmatrix} P_t^2 \rho_{11}(0) & P_t \rho_{10}(0) \\ P_t \rho_{01}(0) & \rho_{00}(0) + \rho_{11}(0)(1 - P_t^2) \end{pmatrix}, \tag{18}$$

with

$$P_t = e^{-\frac{\lambda t}{2}} \left(\cosh\left(\frac{gt}{2}\right) + \frac{\lambda}{g} \sinh\left(\frac{gt}{2}\right) \right). \tag{19}$$

For a qubit in isolation, the evolution can be described by the unitary operator $U(t)$,

$$U(t) = \exp\left(-i \int H_s(t) dt\right), \tag{20}$$

as a solution to Schrödinger equation,

$$|\psi_{cs}(t)\rangle = U(t) |\psi_{cs}(0)\rangle . \tag{21}$$

Integrating the Hamiltonian H_S we obtain

$$U(t) = \begin{pmatrix} \cos(E_0 t) - i\sin(E_0 t) & 0 \\ 0 & \cos(E_0 t) + i\sin(E_0 t) \end{pmatrix}, \tag{22}$$

with,

$$E_0 = \frac{1}{2}\hbar\omega_0. \tag{23}$$

And the state for the isolated qubit is

$$\rho_{cs}(t) = U(t)\rho(0)U(t)^\dagger = \begin{pmatrix} \rho_{11}(0) & Z_t\rho_{10}(0) \\ Z_t^*\rho_{01}(0) & \rho_{00}(0) \end{pmatrix}, \tag{24}$$

with

$$Z_t = \cos^2(E_0 t) - \sin^2(E_0 t) - 2i\sin(E_0 t)\cos(E_0 t). \tag{25}$$

3. Entanglement of Tripartite System

3.1. Dynamics of Three-Qubits State

From the obtained dynamical state for each interacting (18) and isolated qubit (24), the total composite state for three-qubit according to each environment models, Figure 1, can be calculated. We shall follow the procedure proposed in [7] to obtain the state for a system of three non-interacting qubits. The density matrix element for a single qubit can be written as

$$\rho^N_{i_N i'_N}(t) = \sum_{l_N l'_N} A^{l_N l'_N}_{i_N i'_N}(t)\rho^N_{l_N l'_N}(0), \tag{26}$$

$A^{l_N l'_N}_{i_N i'_N}$ is matrix element of Krauss operator with $N = a, b, c$ and $i, i', l, l' = 0, 1$. The reduced density matrix element for three non-interacting qubits is correspondingly expressed by

$$\rho_{i_a i'_a i_b i'_b i_c i'_c}(t) = \sum_{l_a l'_a}\sum_{l_b l'_b}\sum_{l_c l'_c} A^{l_a l'_a}_{i_a i'_a}(t)A^{l_b l'_b}_{i_b i'_b}(t)A^{l_c l'_c}_{i_c i'_c}(t)\rho_{l_a l'_a l_b l'_b l_c l'_c}(0). \tag{27}$$

For example, the element $\langle 111|\,\rho(t)\,|111\rangle = \rho_{111111}(t)$ for 3-cavity models can be obtained using equation (27) as follows

$$\rho^{3-cavity}_{111111}(t) = \sum_{l_a l'_a}\sum_{l_b l'_b}\sum_{l_c l'_c} A^{l_a l'_a}_{1_a 1'_a}(t)A^{l_b l'_b}_{1_b 1'_b}(t)A^{l_c l'_c}_{1_c 1'_c}(t)\rho_{l_a l'_a l_b l'_b l_c l'_c}(0). \tag{28}$$

In Figure 1a, all three qubits interact with their environment and each qubit dynamics is

$$\begin{aligned}
\rho^{(a)}_S(t) &= \begin{pmatrix} P_t^{2^{(a)}}\rho^{(a)}_{11}(0) & P^{(a)}_t\rho^{(a)}_{10}(0) \\ P^{(a)}_t\rho^{(a)}_{01}(0) & \rho^{(a)}_{00}(0) + \rho^{(a)}_{11}(0)(1 - P_t^{2^{(a)}}) \end{pmatrix}, \\
\rho^{(b)}_S(t) &= \begin{pmatrix} P_t^{2^{(b)}}\rho^{(b)}_{11}(0) & P^{(b)}_t\rho^{(b)}_{10}(0) \\ P^{(b)}_t\rho^{(b)}_{01}(0) & \rho^{(b)}_{00}(0) + \rho^{(b)}_{11}(0)(1 - P_t^{2^{(b)}}) \end{pmatrix}, \\
\rho^{(c)}_S(t) &= \begin{pmatrix} P_t^{2^{(c)}}\rho^{(c)}_{11}(0) & P^{(c)}_t\rho^{(c)}_{10}(0) \\ P^{(c)}_t\rho^{(c)}_{01}(0) & \rho^{(c)}_{00}(0) + \rho^{(c)}_{11}(0)(1 - P_t^{2^{(c)}}) \end{pmatrix}.
\end{aligned} \tag{29}$$

From qubit a density matrix, we shall obtain $A^{l_a, l'_a}_{j_a, j'_a}(t)$ term. Expand equation (26) for qubit a

$$\rho^{j_a, j'_a}_S(t) = A^{0_a, 0_a}_{j_a, j'_a}(t)\rho^{(a)}_{0_a, 0_a}(0) + A^{0_a, 1_a}_{j_a, j'_a}(t)\rho^{(a)}_{0_a, 1_a}(0) + A^{1_a, 0_a}_{j_a, j'_a}(t)\rho^{(a)}_{1_a, 0_a}(0) + A^{1_a, 1_a}_{j_a, j'_a}(t)\rho^{(a)}_{1_a, 1_a}(0). \tag{30}$$

Compare equation (29) with equation (30) for element $(1_a, 1_a)$ then it follows

$$A^{0_a,0_a}_{1_a,1_a}(t) = A^{0_a,1_a}_{1_a,1_a}(t) = A^{1_a,0_a}_{1_a,1_a}(t) = 0, \qquad A^{1_a,1_a}_{1_a,1_a}(t) = P_t^{2^{(a)}}, \tag{31}$$

and for elements $(1_a, 0_a)$, $(0_a, 1_a)$, and $(0_a, 0_a)$ we obtained

$$\begin{aligned} A^{0_a,0_a}_{1_a,0_a}(t) = A^{0_a,1_a}_{1_a,0_a}(t) = A^{1_a,1_a}_{1_a,0_a}(t) = 0, \qquad A^{1_a,0_a}_{1_a,0_a}(t) = P_t^{(a)}, \\ A^{0_a,0_a}_{0_a,1_a}(t) = A^{1_a,0_a}_{0_a,1_a}(t) = A^{1_a,1_a}_{0_a,1_a}(t) = 0, \qquad A^{0_a,1_a}_{0_a,1_a}(t) = P_t^{(a)}, \\ A^{0_a,1_a}_{0_a,0_a}(t) = A^{1_a,0_a}_{0_a,0_a}(t) = 0, \qquad A^{0_a,0_a}_{0_a,0_a}(t) = 1, \qquad A^{1_a,1_a}_{0_a,0_a}(t) = 1 - P_t^{2^{(a)}}. \end{aligned} \tag{32}$$

Using the same method, we obtain identical non zero terms of $A^{l_N,l'_N}_{j_N,j'_N}(t)$ for qubit b and c,

$$\begin{aligned} A^{1_b,1_b}_{1_b,1_b}(t) = P_t^{2^{(b)}}, \quad A^{1_b,0_b}_{1_b,0_b}(t) = P_t^{(b)}, \quad A^{0_b,1_b}_{0_b,1_b}(t) = P_t^{(b)}, \\ A^{0_b,0_b}_{0_b,0_b}(t) = 1, \quad A^{1_b,1_b}_{0_b,0_b}(t) = 1 - P_t^{2^{(b)}}, \\ A^{1_c,1_c}_{1_c,1_c}(t) = P_t^{2^{(c)}}, \quad A^{1_c,0_c}_{1_c,0_c}(t) = P_t^{(c)}, \quad A^{0_c,1_c}_{0_c,1_c}(t) = P_t^{(c)}, \\ A^{0_c,0_c}_{0_c,0_c}(t) = 1, \quad A^{1_c,1_c}_{0_c,0_c}(t) = 1 - P_t^{2^{(c)}}. \end{aligned} \tag{33}$$

And substitute results (31-33) to equation (28),

$$\begin{aligned} \rho^{3-cavity}_{111111}(t) &= \sum_{l_a,l'_a}\sum_{l_b,l'_b} A^{l_a,l'_a}_{1_a,1_a}(t) \times A^{l_b,l'_b}_{1_b,1_b}(t) \times \left(A^{1_c,1_c}_{1_c,1_c}(t)\rho_{l_a l'_a l_b l'_b 11}(0)\right), \\ &= \sum_{l_a,l'_a} A^{l_a,l'_a}_{1_a,1_a}(t) \times \left(A^{1_b,1_b}_{1_b,1_b}(t) A^{1_c,1_c}_{1_c,1_c}(t)\rho_{l_a l'_a 1111}(0)\right), \\ &= A^{1_a,1_a}_{1_a,1_a}(t) A^{1_b,1_b}_{1_b,1_b}(t) A^{1_c,1_c}_{1_c,1_c}(t)\rho_{111111}(0), \\ &= P_t^{2^{(a)}} P_t^{2^{(b)}} P_t^{2^{(c)}} \rho_{111111}(0). \end{aligned} \tag{34}$$

Each dynamic of density matrix element for 3-cavity models can be obtained with the same procedure. And by changing each qubit dynamics, equation (29), the evolution of density matrix element for different environment models can also be calculated.

To specify the limit of this study and present the dynamical density matrix for each model in a closed-form we impose an initial condition of the qubits system to be a maximally entangled Agrawal-Pati W state mentioned in [10]. Agrawal-Pati W state is a class of W state that can be used as a resource for teleportation and superdense coding algorithm, which has the following shape [10]

$$|W_n\rangle = \frac{1}{\sqrt{2+2n}}(|100\rangle + \sqrt{n}\,|010\rangle + \sqrt{n+1}\,|001\rangle). \tag{35}$$

Using a class of W state as the initial condition, following procedure (28-34), the dynamical density matrix for all three environment models have a general form of

$$\rho(t) = \begin{pmatrix} 0 & 0 & 0 & 0 & 0 & 0 & 0 & 0 \\ 0 & 0 & 0 & 0 & 0 & 0 & 0 & 0 \\ 0 & 0 & 0 & 0 & 0 & 0 & 0 & 0 \\ 0 & 0 & 0 & \rho_{44}(t) & 0 & \rho^*_{64}(t) & \rho^*_{74}(t) & 0 \\ 0 & 0 & 0 & 0 & 0 & 0 & 0 & 0 \\ 0 & 0 & 0 & \rho_{64}(t) & 0 & \rho_{66}(t) & \rho^*_{76}(t) & 0 \\ 0 & 0 & 0 & \rho_{74}(t) & 0 & \rho_{76}(t) & \rho_{77}(t) & 0 \\ 0 & 0 & 0 & 0 & 0 & 0 & 0 & \rho_{88}(t) \end{pmatrix}, \tag{36}$$

here we have used the computational basis

$$\begin{aligned} |111\rangle = |1\rangle\,, \quad |110\rangle = |2\rangle\,, \quad |101\rangle = |3\rangle\,, \\ |100\rangle = |4\rangle\,, \quad |011\rangle = |5\rangle\,, \quad |010\rangle = |6\rangle\,, \\ |001\rangle = |7\rangle\,, \quad |000\rangle = |8\rangle\,. \end{aligned} \tag{37}$$

3.2. Entanglement Measure

In studying the entanglement dynamics of a system consisting of non-interacting parts described by the Hamiltonian (1), one needs to quantify the entanglement. There is no general and analytical entanglement measure for a multipartite mixed quantum state [11]. However, using entanglement criterion, monogamy inequality of the entanglement for multipartite state exists [12]. From this inequality, a lower bound can be found to give an operational and useful method of quantifying entanglement. One that will be used in this paper is the proposal by Li et al. [8] that calculates lower bound concurrence for arbitrary tripartite mixed states using bipartite entanglement of formation as a foundation.

For a general three-qubit pure state $|\Psi\rangle = \sum_{i,j,k=1} a_{ijk}\,|ijk\rangle$, the concurrence is given by [13]

$$C_3(|\Psi\rangle) = \sqrt{\frac{1}{3}(3 - (Tr(\rho_1^2) + Tr(\rho_2^2) + Tr(\rho_3^2)))}, \tag{38}$$

with $\rho_i = tr_{jk}(\rho)$, $i \neq j \neq k$, and $i = 1, 2, 3$. Any mixed state ρ can be decomposed into an ensemble of pure states $\rho = \sum_j p_j\,|\Psi_j\rangle\,\langle\Psi_j|$, and the concurrence of ρ is then the convex roof of all possible decomposition

$$C_3(\rho) = \inf \sum_j p_j C_3(|\Psi_j\rangle). \tag{39}$$

The minimization procedure to obtain (39) is a high dimensional optimization problem and generally is difficult because of the many possible pure states that can be used to construct the mixed state. Instead of solving this optimization problem numerically, Li et al. proposed a theorem and proof to express its lower boundary that gives rise to genuine multipartite entanglement measures [8]. For an arbitrary three-qubit mixed state, its concurrence lower bound follows

$$C_{LBC}(\rho) = \sqrt{\frac{1}{3}\sum_{l=1}^{6}(C_j^{12|3})^2 + (C_j^{13|2})^2 + (C_j^{23|1})^2}, \tag{40}$$

where

$$C_j^{12|3} = \max\left\{0, \sqrt{\lambda^{12|3}(1)} - \sum_{j>1}^{4}\sqrt{\lambda^{12|3}(j)}\right\}, \tag{41}$$

with $\lambda^{12|3}(j)$ are the eigenvalues of $\rho\tilde{\rho}_j^{12|3}$ in decreasing order. The operator $\tilde{\rho}_j^{12|3}$ is defined by $\tilde{\rho}_j^{12|3} = S_j^{12|3}\rho^* S_j^{12|3}$, and $S_j^{12|3} = (L_j^{12} \bigotimes L^3)$ with L_j^{12} is the j-th generator of $SO(4)$ acting on qubits *1* and *2*, and L^3 is the generator of $SO(2)$ acting on qubit *3*, or $L^3 = \sigma_y^3$ where σ_y is the Y Pauli matrix. $C_j^{13|2}$ and $C_j^{23|1}$ are defined similarly. Evaluating the general form of the dynamical density matrix obtained in equation (36) with concurrence lower bound we get the analytical expression of its entanglement value as

$$C_{LBC}(\rho) = \sqrt{\frac{4}{3}\Big[(\max\{0, |\rho_{74}(t)|\})^2 + (\max\{0, |\rho_{76}(t)|\})^2 + (\max\{0, |\rho_{64}(t)|\})^2\Big]}. \tag{42}$$

Moreover, it has been shown in [14] that the lower bound concurrence method by Li et al. coincides with the result from the numerical method for solving the convex roof problem (39) for density matrices with rank ≤ 4. And as we obtained earlier, the exact dynamical density matrix in the scope of this study (36) has a maximum rank of 4 and hence this method can be used.

4. Result and Discussion

In this section, we will investigate the entanglement dynamics of qubits following the procedure and measure introduce in the previous section. The dependency of C_{LBC} (42) on $|\rho_{64}(t)|^2$, $|\rho_{74}(t)|^2$, and $|\rho_{76}(t)|^2$ deppends on the dynamical function P_t. The function P_t has two distinctly different behaviour that depends on the value of g (17). When g is a real number or $\lambda/\gamma_0 > 2$, P_t is an exponentially decaying function whereas if g is an imaginary number or $\lambda/\gamma_0 < 2$, P_t is describing an oscillatory function. These different behaviours can be correlated with the non-Markovian and Markovian processes by the environment. Markovian approximation, $\tau_R \ggg \tau_B$, can perfectly describe the dynamics of open quantum systems under fast dynamics as the Lindblad master equation. With the connection between characteristic time and systems parameter as follows,

$$\frac{\lambda}{\gamma_0} \propto \frac{\tau_R}{\tau_B}. \tag{43}$$

the Markovian process corresponds with exponentially decaying behaviour of P_t. While the more general non-Markovian process, without the Markovian approximation, corresponds to the oscillatory function of P_t with $\lambda/\gamma_0 = 2$ as a boundary between the two processes. The physical interpretation of the non-Markovian process is sometimes described as having non-trivial memory or feedback from the environment to the system.

The three-dimensional graphs in Figure 2 show the value of C_{LBC} as a function of a dimensionless parameter $\gamma_0 t$ and λ/γ_0. Setting the parameter λ/γ_0 to the corresponding values for Markovian/non-Markovian regime, one gets the two-dimensional graphs of Figure. 2. For all of the three models, the C_{LBC} exhibits exponential decay behavior in the Markovian regime with λ/γ_0 as the decay constant until it reaches a stationary value. For the 1-cavity system in Figure 2f, this value is a constant. Meanwhile, for the other two cases, the stationary value is asymptotically zero. In the non-Markovian regime, all the three models give the same stationary value as in the Markovian regime for $t \to \infty$.

In the non-Markovian regime, the C_{LBC} of the 3-cavity in Figure 2b displays damped oscillatory behavior. In contrast, the 2-cavity system in Figure 2d saw alternating patterns of two damped oscillators, which is expected given the in-homogeneity qubit-environment coupling in the 2-cavity models contrary to the 3-cavity. We will call the larger damped oscillatory pattern in the two-cavity system primary and the smaller one secondary. The entanglement value of the primary damped oscillator comes from the contribution of both coupled-isolated and coupled-coupled qubits pair. While the secondary damped oscillators correspond with the dark periods between the entanglement revival of coupled-isolated qubits pair that causing the entanglement value contribution comes only from the entanglement between the two environmentally coupled qubits. For both of the models with the same value of λ/γ_0, because of the entanglement alternating patterns, the decay of C_{LBC} for the 2-cavity model is not as fast as the 3-cavity model. The oscillatory behaviour of the entanglement shows the characteristic entanglement revival of the non-Markovian process. Stationary values of both models are asymptotically zero, which means that the three qubits will disentangle in a finite time such that $C(\rho) \approx 0$. But compared to their Markovian regime in respective models, the non-Markovian regime extends the time of entanglement because of the revival phenomenon.

For the 1-cavity model, the entanglement does not disappear completely because of the non-zero stationary value. Qubits a and c are in isolation with the bipartite entanglement between

them is a non-zero constant. For a class of W state, as qubit b interacts with cavity and disentangle with qubit a and c (partially trace b subsystems), the other two qubits will still be entangled [15]. The concurrence between qubit a and c is then contribute to the C_{LBC} as a minimum or the stationary value when $t \to \infty$. Figure 2f also shows pseudo-dark-periods (non-zero value) between the revival of entanglement, which contribute to slower entanglement decay.

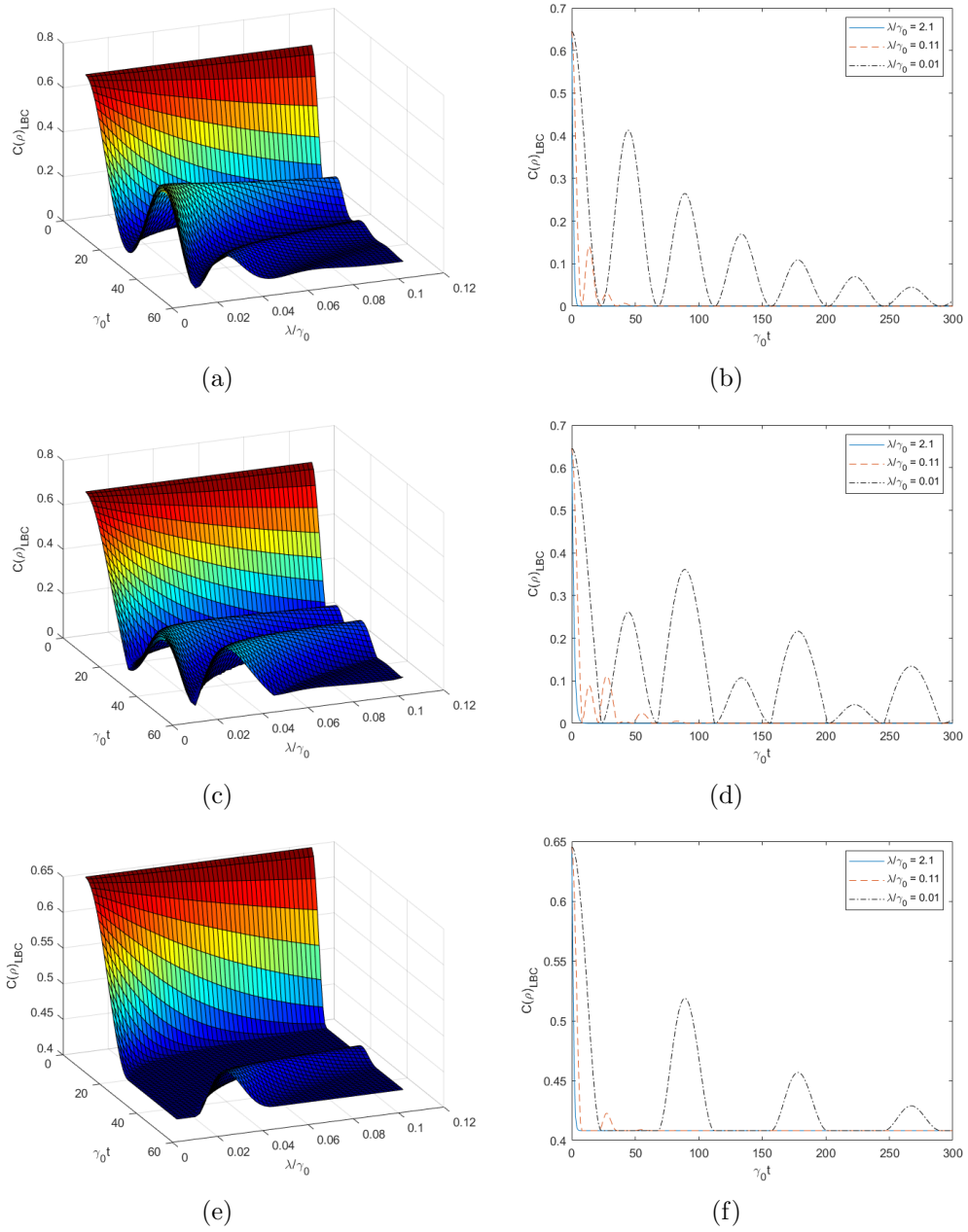

Figure 2: The $C_{LBC}(\rho)$, $n = 1$, for (a) 3-cavity, (c) 2-cavity, and (e) 1-cavity model. And two-dimensional projection of (b) 3-cavity, (d) 2-cavity, (f) 1-cavity model setting the value of $\lambda/\gamma_0 = 2.1$ (solid blue line) for Markovian regime, $\lambda/\gamma_0 = 0.1$ (dashed red line) for experimental value of QED cavity, and $\lambda/\gamma_0 = 0.001$ (dot-dashed black line) for non-Markovian regime.

5. Conclusion

In summary, the entanglement dynamics of an atomic-cavity system consisting of three qubits initially prepared as a class of W state with different environment model was investigated. Total dynamics of the systems are calculated using the Bellomo procedure and governed by each qubit dynamic (26-27). We solved the system evolution of multiple environment schemes in Figure 1, measure their entanglement evolution analytically using lower bound concurrence (42), and visualize the result using graphs in Figure 2.

Without using Markovian approximation, the calculation is valid for both Markovian and non-Markovian processes with the systems parameter λ/γ_0 define the respective regime. In the Markovian regime, the evolution of LBC displays the usual decaying behaviour as in the GKSL master equation [16]. In the non-Markovian regime, we observe the revival of entanglement that depends on the structure of qubits bipartition. We also found the dark period of entanglement revival in the non-Markovian regime which prolongs entanglement time compared to the Markovian process. We also show that for the 3-cavity and 2-cavity models, even though both models always lead to disentangled states, the 2-cavity model is more robust because the disentanglement time is relatively longer. This is consistent with what one would expect about the relation between the amount of exposure to the environment and the decoherence time.

Acknowledgment

The authors express their gratitude to Institut Teknologi Bandung (ITB) that supported this work through "Penelitian, Pengabdian Kepada Masyarakat, dan Inovasi Kelompok Keahlian (PPMI KK) ITB 2021" program.

References

[1] Nielsen M and Chuang I 2000 *Quantum Computation and Quantum Information* (Cambridge: Cambridge University Press)
[2] Wootters W K 1998 *Philos. Trans. R. Soc.* A **356** 1717–1731
[3] Hsieh M H, Devetak I and Brun T 2007 *Phys. Rev.* A **76** 062313
[4] Shen C, Noh K, Albert V V, Krastanov S, Devoret M H, Schoelkopf R J, Girvin S M and Jiang L 2017 *Phys. Rev.* B **95**(13) 134501
[5] Cottet A, Dartiailh M C, Desjardins M M, Cubaynes T, Contamin L C, Delbecq M, Viennot J J, Bruhat L E, Douçot B and Kontos T 2017 *J. Phys. Condens. Matter* **29** 433002
[6] Yamasaki H, Pirker A, Murao M, Dür W and Kraus B 2018 *Phys. Rev.* A **98** 052313
[7] Bellomo B, Lo Franco R and Compagno G 2008 *Phys. Rev.* A **77** 032342
[8] Li M, Fei S M, Li-Jost X and Fan H 2015 *Phys. Rev.* A **92** 062338
[9] An N B, Kim J and Kim K 2011 *Phys. Rev.* A **84**(2) 022329
[10] Agrawal P and Pati A 2006 *Phys. Rev.* A **74** 062320
[11] Aolita L, de Melo F and Davidovich L 2015 *Rep. Prog. Phys.* **78** 042001
[12] Ou Y C, Fan H and Fei S M 2008 *Phys. Rev.* A **78** 012311
[13] Li M, Fei S M and Wang Z X 2009 *J. Phys.* A **42** 145303
[14] Siomau M and Fritzsche S 2010 *Eur. Phys. J.* D **60** 397–403
[15] Dür W, Vidal G and Cirac J I 2000 *Phys. Rev.* A **62** 062314
[16] Manzano D 2020 *AIP Adv.* **10** 025106